



移动阅读

石柱, 夏国清, 郝夏炜, 等, 2025. 青藏高原沱沱河盆地始新世—中新世湖相碳酸盐岩碳氧同位素特征与古环境意义[J]. 沉积与特提斯地质, 45(2): 233–248. doi: 10.19826/j.cnki.1009-3850.2024.07005

SHI Z, XIA G Q, HAO X W, et al., 2025. Carbon and oxygen isotopic composition and palaeoenvironment characteristics of Eocene–Miocene lacustrine carbonate rocks in the Tuotuohe Basin, Qingzang (Tibet) Plateau[J]. Sedimentary Geology and Tethyan Geology, 45(2): 233–248. doi: 10.19826/j.cnki.1009-3850.2024.07005

## 青藏高原沱沱河盆地始新世—中新世湖相碳酸盐岩碳氧同位素特征与古环境意义

石柱<sup>1,2</sup>, 夏国清<sup>1,2\*</sup>, 郝夏炜<sup>1,2</sup>, 李高杰<sup>3</sup>, 迪力夏提·艾海提<sup>4</sup>

(1. 成都理工大学油气藏地质及开发工程国家重点实验室, 四川 成都 610059; 2. 成都理工大学沉积地质研究院, 四川 成都 610059; 3. 绵阳师范学院资源环境工程学院, 四川 绵阳 621000; 4. 新疆维吾尔自治区地质矿产勘查开发局第九地质大队, 新疆 乌鲁木齐 830000)

**摘要:** 沱沱河盆地位于青藏高原腹地, 是感应高原隆升过程及环境变化效应的核心地带, 其内部新生代沉积地层记录了高原地形地貌演化过程及环境、气候变迁的信息。原生湖相碳酸盐岩沉积与区域环境变化关系密切, 它的碳氧同位素特征及组合是研究古环境和古气候变化的重要指标。在青藏高原北部沱沱河盆地新生代湖相碳酸盐岩岩石学和矿物学分析基础上, 开展了碳氧同位素特征研究, 并探讨了古环境意义。结果表明: 沱沱河盆地新生代湖相碳酸盐岩主要为泥微晶灰岩, 以及少量白云岩和含生物碎屑泥晶灰岩, 垂向上, 碳氧同位素组成特征揭示该区古环境存在四个演化阶段: 第一阶段对应于38.5~30.5 Ma时期, 该时期湖相碳酸盐岩形成于气候相对湿润的开放型湖泊, 是冲积扇—河流相干旱气候背景下短暂性雨水输入至洪泛平原内部湖盆所致; 第二阶段对应于30.5~23.6 Ma, 且该阶段26.5 Ma前后的古环境存在明显变化, 30.5~26.5 Ma时期, 气候相对湿润, 但区域降水量减少, 蒸发作用加强, 与高原北部局部隆升及湖盆水文状态发生改变有关, 26.5~23.6 Ma时期蒸发作用相对增加, 气候干冷, 是青藏高原北部地区地貌格局发生转变、西风带降水输入减少所致; 第三阶段(23.6~22.3 Ma)盆地蒸发作用相对降低, 气候相对湿润, 与青藏高原腹地发育古大湖有关; 第四阶段(22.3~19.7 Ma)气候更加干冷, 湖泊类型转变为封闭型咸水湖, 为可可西里地区进入高原系统和亚洲内陆干旱化导致。沱沱河盆地始新世—中新世湖相碳酸盐岩碳氧同位素所揭示的湖泊水文状态和气候背景的转变与高原北部古地理格局和地貌演化存在极大关联。

**关键词:** 始新世—中新世; 湖相碳酸盐岩; 碳氧同位素; 古环境; 青藏高原

中图分类号: P597

文献标识码: A

## Carbon and oxygen isotopic composition and palaeoenvironment characteristics of Eocene–Miocene lacustrine carbonate rocks in the Tuotuohe Basin, Qingzang (Tibet) Plateau

SHI Zhu<sup>1,2</sup>, XIA Guoqing<sup>1,2\*</sup>, HAO Xiawei<sup>1,2</sup>, LI Gaojie<sup>3</sup>, Dilixiati·Aihaiti<sup>4</sup>

(1. State Key Laboratory of Oil and Gas Reservoir Geology and Exploitation, Chengdu University of Technology, Chengdu 610059, China; 2. Institute of Sedimentary Geology, Chengdu University of Technology, Chengdu 610059, China; 3. College of

收稿日期: 2024-01-30; 改回日期: 2024-03-13; 责任编辑: 周小琳

作者简介: 石柱(1998—), 男, 硕士研究生, 地质学专业。E-mail: shizhu160103@163.com

通信作者: 夏国清(1982—), 男, 教授, 博士生导师, 主要从事沉积学的教学和科研工作。E-mail: xiaguqing2012@cdut.cn

资助项目: 国家自然科学基金“青藏高原新生代湖相碳酸盐岩碳氧同位素特征与古环境意义”(41972115)

*Resources and Environmental Engineering, Mianyang Normal University, Mianyang 621000, China; 4. No. 9 Geological Party, Xinjiang Bureau of Geological and Mining Resources, Urumqi 830000, China)*

**Abstract:** The Tuotuohe Basin, located in the Qingzang (Tibet) Plateau, is one of the core areas that attested to predominant environmental changes during the plateau's uplift. The Cenozoic sedimentary successions in this region record the evolution of the plateau's topography and geomorphology, as well as regional climatic changes. Based on the petrological and mineralogical analysis of Cenozoic lacustrine carbonate rocks in the Tuotuohe Basin, the characteristics of carbon and oxygen isotopes are studied to explore their paleoenvironmental significance. The results show that the Cenozoic lacustrine carbonate rocks in the Tuotuohe Basin are dominated by micritic limestone, with a small amount of dolomite and bioclastic limestone. The vertical carbon and oxygen isotopic compositions reveal four stages of paleoenvironmental evolution in this area: The first stage corresponds to the period of 38.5-30.5 Ma, when lacustrine carbonate rocks formed in an open lake during a relatively humid climate, likely influenced by increased rainwater input to the lake basin in a flood plain setting under the background of alluvial fan-fluvial drought climate. The second stage is from 30.5 Ma to 23.6 Ma, during which there were significant changes in the paleoenvironment around 26.5 Ma. From 30.5 Ma to 26.5 Ma, the climate was relatively humid, but regional precipitation decreased, and evaporation intensified, related to the local uplift in the northern part of the plateau and changes in the lake basin's hydrological status. From 26.5 Ma to 23.6 Ma, increased evaporation and a dry, cold climate resulted from the change of geomorphic framework in the northern Qingzang (Tibet) Plateau and the reduced westerly rain input. The third stage is between 23.6 Ma and 22.3 Ma, when evaporation decreased, and the climate became relatively humid, related to the development of ancient lakes in the hinterland of the Qingzang (Tibet) Plateau. In the fourth stage (22.3 Ma-19.7 Ma), the climate became drier and colder, and the lake transitioned to a closed saltwater lake, caused by the integration of Hoh Xil into the plateau system and the drying of the interior of Asia. The changes in lake hydrology and climate, revealed by the carbon and oxygen isotopes of the Eocene-Miocene lacustrine carbonate rocks in the Tuotuohe Basin, are closely related to the paleogeographic pattern and geomorphologic evolution in the northern part of the plateau.

**Key words:** Eocene-Miocene; lacustrine carbonate rock; carbon and oxygen isotope; palaeoenvironment; Qingzang (Tibet) Plateau

## 0 引言

青藏高原新生代构造隆升不仅造就了亚洲古地形地貌的改变,奠定了今日东亚山川水系格局,同时也导致全球气候体系的完全改变,催生了地球上强大的季风环流,并在中国西北部形成巨大的内陆干旱区(钟大赉和丁林, 1996; 刘东生等, 1998; 施雅风等, 1998; 李吉均, 1999; An et al., 2001; 肖国桥等, 2014; 孙继敏等, 2017)。因此,青藏高原研究不但是国际地球科学研究的前沿领域,而且是全球环境变化研究普遍关注的问题。青藏高原腹地是直接感应高原隆升过程环境变化效应的核心地带,这里的山间盆地不仅能够记录大陆碰撞过程、岩石圈和地壳变形历史,同时也是获取高原地形地貌演化过程及环境、气候变迁信息最理想的场所(Wang et al., 2008; Li et al., 2014; 吴劲宣等, 2022; 包万铖等, 2023; 路畅等, 2023; 汪素凤等, 2023)。

在陆相湖泊环境中,气候变化和构造运动是控制区域环境变化的主要因素。构造隆升所产生的

地形地貌变化直接控制着湖盆形态和陆源碎屑物质输入的数量与速率,而气候的冷暖变化和湿度的干湿波动影响着湖泊环境水文化学平衡状态(伊海生等, 2007)。不同气候区化学沉积物类型及沉积作用方式存在明显差异,例如,在湿润气候区内的湖泊,降雨量充沛,陆源物质输入较多,沉积物以碎屑岩为主,而化学沉积主要是碳酸盐类沉积,且常以夹层形式存在;而在干旱气候背景下的湖泊,湖水蒸发消耗强烈,河流或地下水带来的盐分长期积累在湖泊中,致使湖水盐度增大,转变为咸水湖或盐湖,直至盐湖消失并进入干盐湖阶段(沈吉等, 2010)。因此,湖相碳酸盐岩的形成是特定气候条件下环境水文化学平衡状态变化的结果,是古代沉积盆地环境变化研究的重要载体。

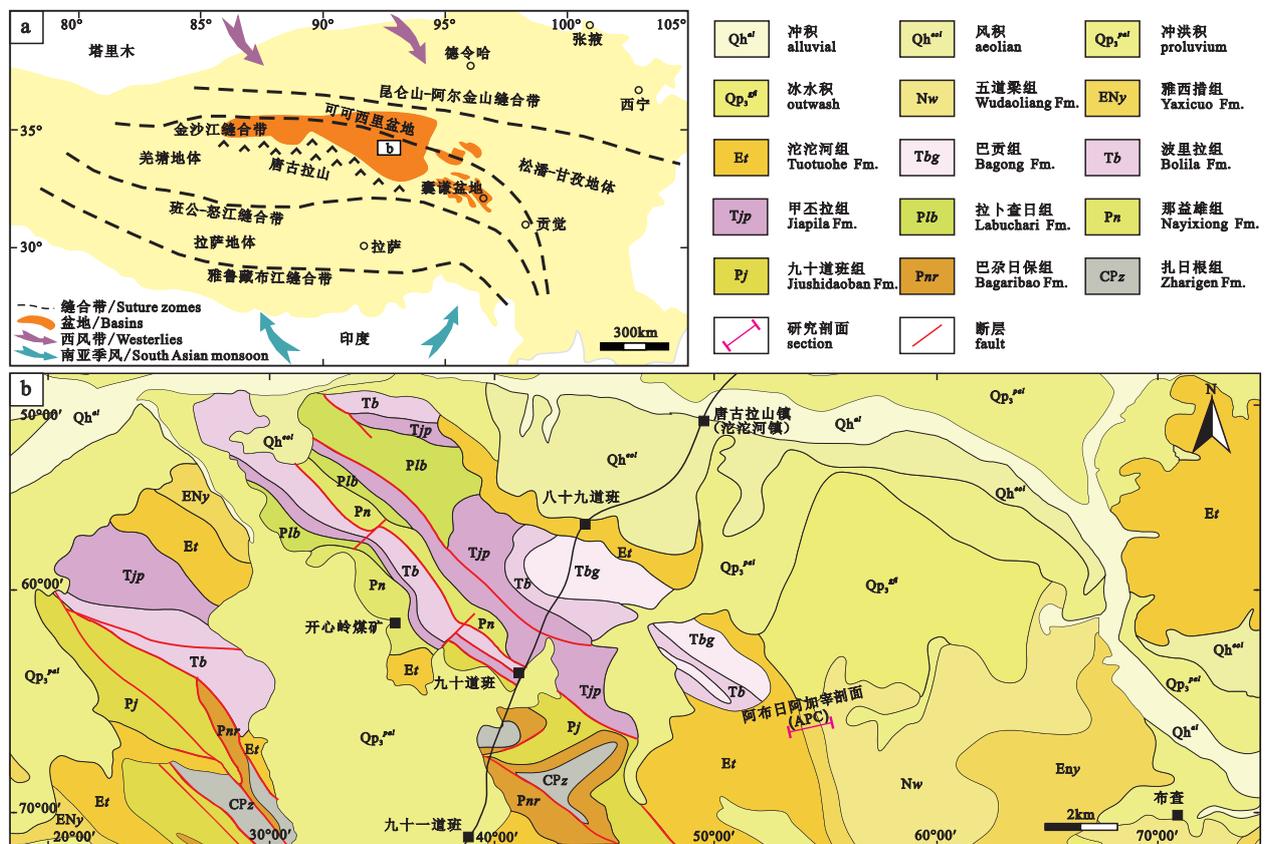
在众多古气候环境指标序列中,碳氧同位素的地球化学方法是判别沉积环境变化的一个重要参数,长期以来在第四纪和现代湖泊学领域得到了广泛的应用(邵龙义和张鹏飞, 1991; Hough et al., 2010; Kämpf et al., 2020; Zeng et al., 2023)。现代湖

泊学研究表明,影响湖相碳酸盐岩碳同位素组成的主要因素是湖水中的溶解无机碳(Hoefs, 1997),其与大气 CO<sub>2</sub> 交换过程中的碳同位素分馏属于动力学过程,在干旱背景下,碳同位素值与蒸发强度表现为正相关关系;而湖泊碳酸盐岩中氧同位素通常与气温、湿度和大气降水的<sup>18</sup>O/<sup>16</sup>O 比值有关,在陆地湖泊体系中,它可能更多地反映湖泊的水文平衡状态,即蒸发量与注入量的变化(Horton et al., 2016)。因此,原生湖相碳酸盐岩沉积与区域环境变化关系密切,它的碳氧同位素特征及组合是研究古环境和古气候变化的重要指标。本研究选择位于青藏高原北部沱沱河盆地阿布日阿加宰(APC)剖面始新世至中新世湖相碳酸盐岩为研究对象,分析其碳氧同位素组成及变化特征,结合宏观沉积环境分析,揭示其成因与古环境信息,为高原演化历史和环境变化过程研究提供依据。

### 1 区域地质概况与剖面特征

沱沱河盆地位于青藏高原北部腹地(图 1a),

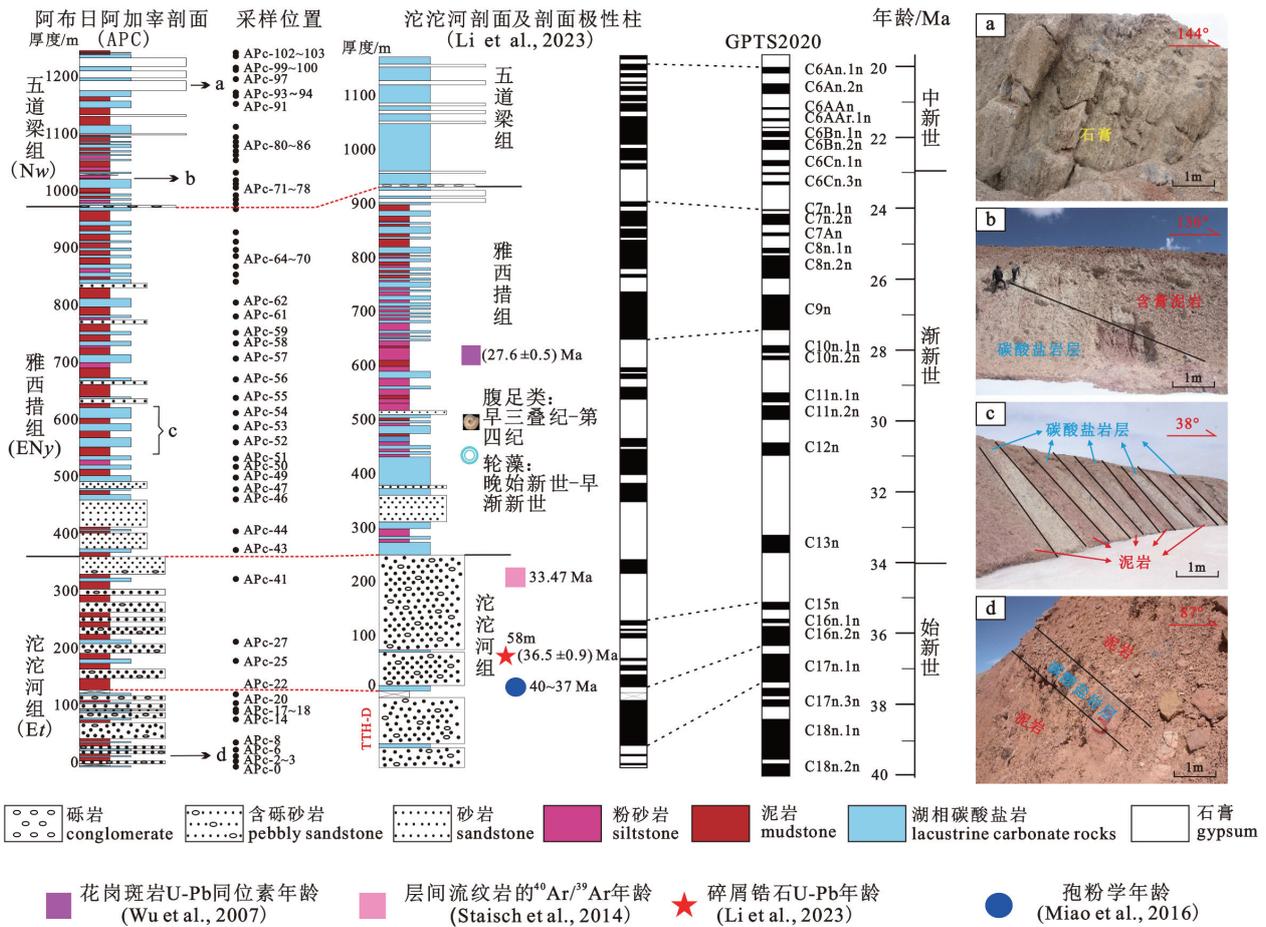
是可可西里盆地南部次级坳陷。盆地的新生代地层包括三个单元,由下至上依次为沱沱河组、雅西措组、五道梁组(刘志飞等, 2005)。实测地层剖面——阿布日阿加宰(APC)剖面位于盆地中部(34°08'69"N, 92°49'27"E; 图 1b),距唐古拉山镇东南约 15 km。实测地层厚度约 1 244.8 m,依次为沱沱河组、雅西措组和五道梁组地层,均为整合接触(图 2)。底部沱沱河组(厚度 0~363.5 m)由厚层状复成分砾岩、含砾砂岩、砂岩组成,以发育大规模交错层理、沙纹层理、波痕为特征,属山前冲洪积扇相沉积,局部间夹洪泛平原相短暂性湖泊碳酸盐岩沉积;中部雅西措组地层厚度 611.2 m,岩性主要为河流—浅湖相紫红色砂、泥岩,上部薄层状灰白色泥质灰岩较为发育;顶部五道梁组地层厚度 270.1 m,岩性主要为灰白色、灰绿色钙质泥岩、泥灰岩,见大量石膏等蒸发岩沉积,以干盐湖相沉积为特征。对于该剖面地层时代, Li et al.(2023)进行过详细的磁性地层学和同位素年代学研究,将剖面各地层沉积时代限定为:沱沱河组 38.5~32.7 Ma,雅西措组 32.7~



a. 沱沱河盆地大地构造位置 (据 Li et al., 2018 修改); b. 研究区区域地质简图

图 1 沱沱河盆地地质简图及研究剖面位置

Fig. 1 Geological schematic map and study section location of the Tuotuohe Basin



a. 五道梁组发育厚层石膏；b-d. 五道梁组、雅西措组、沱沱河组湖相碳酸盐岩野外宏观照片

图2 沱沱河盆地阿布日阿加宰实测地层剖面特征及地层时代 (据 Li et al., 2023 修改)

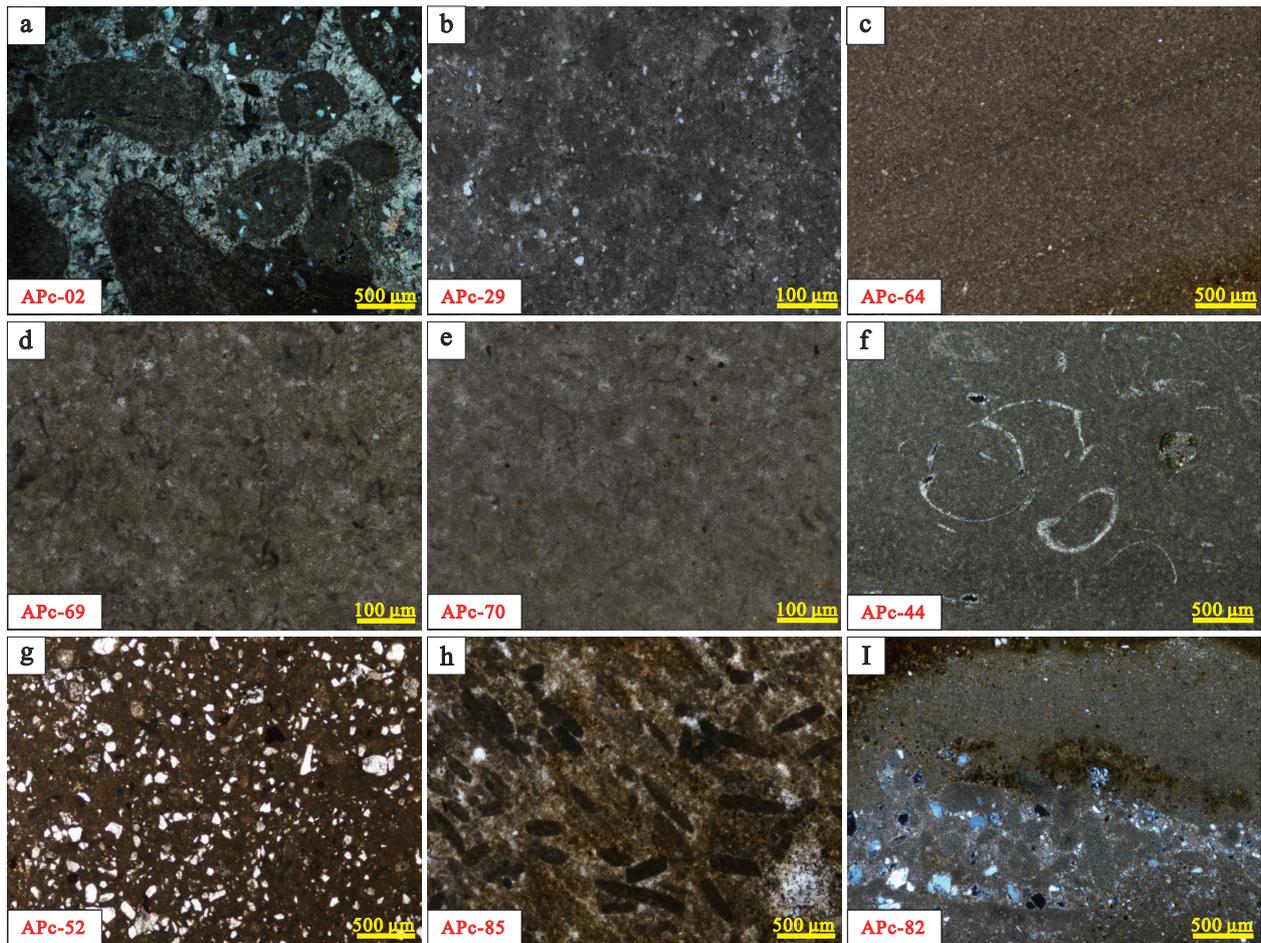
Fig. 2 Measured stratigraphic section at the APC section in the Tuotuohe Basin and its stratigraphic age (modified from Li et al., 2023)

23.6 Ma, 五道梁组 23.6~19.7 Ma(图2)。

## 2 样品采集与实验方法

湖相碳酸盐岩样品分别采自沱沱河组、雅西措组和五道梁组三个地层单元,野外标志显著,均以灰白色、黄灰色色调为主,以薄层状产出为特征,与紫红色砂泥岩层对比鲜明。野外共采集到60层碳酸盐岩样品,其中沱沱河组13件,碳酸盐岩层位于块状复成分砾岩及紫红色岩屑砂岩之上的泥质砂岩层,常以夹层形式出现;雅西措组25件,主要采于以砂岩夹碳酸盐岩或以细碎屑岩—碳酸盐岩—细碎屑岩为主体的旋回性层序中;五道梁组样品22件,五道梁组下部地层中碳酸盐岩层常与紫红色粉砂质泥岩、灰质黏土岩呈不等厚互层产出,上部地层中碳酸盐岩层则主要位于含膏泥岩—碳酸盐岩—含膏泥岩的层序内。除沱沱河组底部2

件样品为古土壤碳酸盐岩结核外(图3a),其余样品均为湖泊相碳酸盐岩沉积。为保证数据的可靠性,野外尽量选择新鲜未经风化的岩石,同时避开含有方解石脉的样品。首先在室内对样品开展岩石学和矿物学研究,在此基础上对样品进行全岩碳氧同位素分析。通过X射线衍射分析对矿物类型进行鉴定,此工作在成都南达微构质检技术服务有限公司实验室完成,仪器为日本理学 Rigaku Ultima IV, CuKα靶,测试电压40 kV,测试电流40 mA,扫描宽度3°~90°,连续扫描,发散狭缝尺度0.6°,接收狭缝为0.1 mm,测量温度25℃,湿度50%。碳氧同位素测定在中国科学院南京地质古生物研究所同位素实验室完成,采用磷酸法,将样品粉碎至200目,经烘干后在真空条件下与无水H<sub>3</sub>PO<sub>4</sub>反应220秒,使用美国 Thermo Finnigan 公司 MAT253 气体同位素质谱仪直接测定产生的CO<sub>2</sub>同位素组



a. 古土壤碳酸盐岩结核, 见泥晶方解石球粒, 球粒间被亮晶方解石填充; b-c. 泥晶灰岩, 主要由泥微晶方解石组成, 见少量半圆状石英颗粒; d-e. 白云岩, 主要由泥晶白云石构成, 含少量沉积成因的石英颗粒; f. 含生物碎屑泥晶灰岩, 生物碎屑以介壳类为主, 形态保存完整; g-i. 泥晶灰岩中见大量陆源碎屑物质, 碎屑以陆源石英颗粒为主

图3 阿布日阿加宰剖面碳酸盐岩镜下特征

Fig. 3 Microscopic characteristics of the lacustrine carbonate rocks in the APC section

成, 实验室室温控制在 25℃。采用 V-PDB (Vienna-Pee Dee Belemnite) 标准, 标样为 GBW04405,  $\delta^{13}\text{C}_{\text{VPDB}} = (+0.57 \pm 0.03)\text{‰}$ ,  $\delta^{18}\text{O}_{\text{VPDB}} = (-8.49 \pm 0.14)\text{‰}$ , 测试精度  $\delta^{13}\text{C}$  为 0.031‰,  $\delta^{18}\text{O}$  为 0.060‰。同时, 实验室随机抽取了 37 件样品开展重复性测试, 确保测试结果的可靠性。

### 3 测试结果

分析结果表明, 沱沱河盆地新生代湖相碳酸盐岩主要为泥微晶灰岩(图 3b-c)以及少量白云岩和含生物碎屑泥晶灰岩, 岩石中未发现亮晶方解石或重结晶等具有明显成岩蚀变特征的矿物, 表明研究剖面的碳酸盐矿物受成岩作用的影响较小; 同时观察发现白云岩中白云石晶体较小(图 3d-e), 泥晶结构, 半自形—自形, 未见后期交代成因结构; 生物碎

屑泥晶灰岩中生物碎屑以介壳类为主, 形态保持完好(图 3f); 少量样品碎屑组分含量较高, 碎屑以石英和内碎屑为主(图 3g-h), 部分碎屑物质呈纹层状产出(图 3i)。X 射线衍射(X-ray diffraction, XRD)分析得到样品中碳酸盐岩矿物以方解石为主(含量最高为 97.3%, 平均 41.12%), 少量白云石(含量普遍小于 15%), 个别样品白云石含量大于方解石(图 4; 表 1)。尽管含少量陆源碎屑, 但前人研究显示, 不同比例的陆源碎屑矿物并不会影响碳氧同位素分析结果(邓文峰等, 2005), 因此这部分样品的碳氧同位素分析结果同样可以用来指示碳酸盐岩沉积时期古湖泊环境与古气候信息。

沱沱河盆地新生代湖相碳酸盐岩碳氧同位素分析结果如下(表 1):  $\delta^{18}\text{O}$  值范围在  $-11.58\text{‰} \sim +1.73\text{‰}$  之间, 平均值为  $-4.95\text{‰}$ ,  $\delta^{13}\text{C}$  值范围在

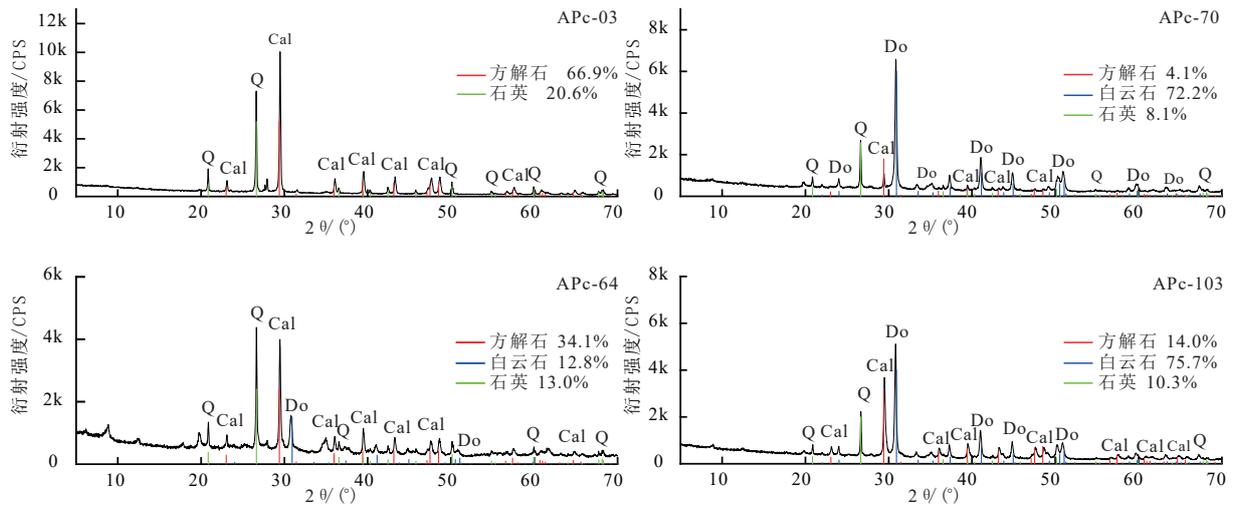


图4 阿布日阿加宰剖面湖相碳酸盐岩矿物鉴定代表性样品 XRD 图

Fig. 4 XRD diagrams of representative samples showing the identification of the lacustrine carbonate rocks in the APC section

表1 沱沱河盆地阿布日阿加宰剖面湖相碳酸盐矿物相对百分含量及碳氧同位素分析结果

Table 1 Relative percentages of carbonate minerals and carbon and oxygen isotope values of lacustrine carbonate rocks in the APC section of the Tuotuohe Basin

地层	样品编号	碳酸盐矿物相对含量		$\delta^{18}\text{O}/\text{‰}$	$\delta^{18}\text{O}/\text{‰}^{\blacktriangle}$	$\delta^{13}\text{C}/\text{‰}$	地层	样品编号	碳酸盐矿物相对含量		$\delta^{18}\text{O}/\text{‰}$	$\delta^{18}\text{O}/\text{‰}^{\blacktriangle}$	$\delta^{13}\text{C}/\text{‰}$
		方解石/%	白云石/%						方解石/%	白云石/%			
沱沱河组	APc-00	100.00	0.00	-10.18	-10.18	5.04	雅西措组	APc-64*	71.03	28.97	-6.13	-6.61	0.58
	APc-02	100.00	0.00	-10.26	-10.26	5.43		APc-65*	70.15	29.85	-5.64	-6.13	0.84
	APc-03**	100.00	0.00	-9.11	-9.11	4.33		APc-66**	70.56	29.44	-5.17	-5.66	0.87
	APc-06**	100.00	0.00	-8.32	-8.32	4.55		APc-67*	65.80	34.20	-4.20	-4.77	1.43
	APc-08	100.00	0.00	-7.05	-7.05	4.64		APc-68**	28.11	71.89	-2.60	-3.80	-0.27
	APc-14	100.00	0.00	-7.72	-7.72	0.97		APc-69	30.39	69.61	-1.61	-2.77	0.42
	APc-17	71.49	28.51	-9.03	-9.50	-0.18		APc-70	4.96	95.04	0.73	-0.86	0.59
	APc-18**	97.44	2.56	-7.82	-7.86	-0.81		APc-71*	72.50	27.50	-2.33	-2.78	1.62
	APc-20	100.00	0.00	-7.93	-7.93	-0.09		APc-72	4.44	95.56	0.31	-1.28	-0.27
	APc-22	100.00	0.00	-8.58	-8.58	0.60		APc-73*	82.45	17.55	-5.68	-5.97	1.52
	APc-25	100.00	0.00	-8.21	-8.21	2.11	APc-74*	86.85	13.15	-5.57	-5.78	0.77	
	APc-27	98.53	1.47	-8.65	-8.68	1.85	APc-75	54.57	45.43	0.12	-0.63	0.40	
	APc-41*	83.63	16.37	-7.83	-8.10	3.71	APc-76*	73.90	26.10	-5.76	-6.19	1.52	
	APc-43*	98.16	1.84	-8.96	-8.99	3.15	APc-77*	83.49	16.51	-4.54	-4.81	0.37	
	APc-44	100.00	0.00	-7.46	-7.46	2.81	APc-78*	75.11	24.89	-1.72	-2.13	-0.51	
	APc-46*	91.21	8.79	-6.65	-6.79	1.53	APc-80*	85.72	14.28	-4.13	-4.36	-0.37	
	APc-47**	53.68	46.32	-7.20	-7.97	1.42	APc-81*	82.14	17.86	-7.58	-7.88	1.23	
	APc-49*	100.00	0.00	-5.12	-5.12	2.27	APc-82	93.00	7.00	1.02	0.90	-1.00	
	APc-50*	100.00	0.00	-6.51	-6.51	0.82	APc-83*	36.92	63.08	-2.71	-3.76	0.48	
	APc-51*	94.31	5.69	1.05	0.96	-2.06	五道梁组	APc-84*	100.00	0.00	-3.81	-3.81	3.46
APc-52**	34.71	65.29	-6.46	-7.54	1.53	APc-85	98.68	1.32	-8.59	-8.61	1.63		
雅西措组	APc-53	89.15	10.85	-3.58	-3.76	1.14	APc-86	60.83	39.17	-4.58	-5.23	0.34	
APc-54**	93.21	6.79	-5.36	-5.47	1.60	APc-91	93.91	6.09	-1.51	-1.61	1.16		
APc-55*	100.00	0.00	-6.17	-6.17	-0.48	APc-93*	27.07	72.93	-3.43	-4.64	-2.47		
APc-56*	100.00	0.00	0.80	0.80	1.19	APc-94*	56.50	43.50	-3.67	-4.39	1.21		
APc-57*	0.00	100.00	-8.80	-10.44	1.03	APc-97*	0.00	100.00	1.73	0.06	1.32		
APc-58**	6.61	93.39	-0.81	-2.36	0.56	APc-99	100.00	0.00	-11.58	-11.58	1.66		
APc-59	11.72	88.28	-2.46	-3.92	1.86	APc-100	50.00	50.00	-2.59	-3.42	0.87		
APc-61	65.98	34.02	1.12	0.55	0.82	APc-102*	100.00	0.00	-5.41	-5.41	1.17		
APc-62*	51.37	48.63	-2.12	-2.93	1.15	APc-103*	0.00	100.00	-0.78	-2.44	-1.67		

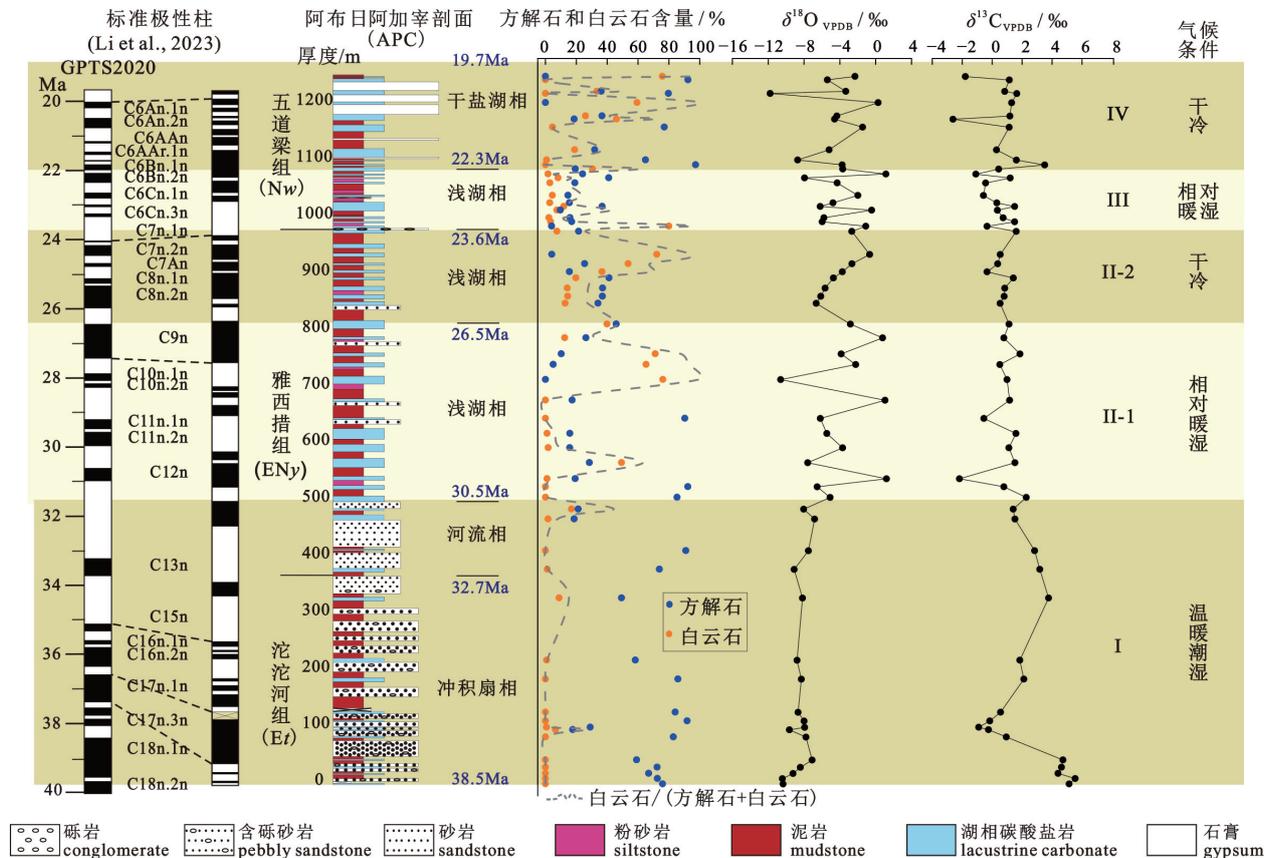
注：表中样品号带“\*”的，表示重复测试样品，“\*”个数代表重复测试次数； $\delta^{18}\text{O}$ 带“▲”的，表示校正后的 $\delta^{18}\text{O}$ 值。

-2.47‰~+5.43‰之间,平均值为+1.13‰。从垂向上看,整个剖面氧同位素值表现为逐渐正偏趋势,而碳同位素值则表现为逐渐负偏的趋势。

#### 4 阿布日阿加宰剖面碳氧同位素变化特征与古环境指示

湖相碳酸盐岩中  $\delta^{18}\text{O}$  值主要取决于当时湖水中  $\delta^{18}\text{O}$  值与湖水温度,而湖水中  $\delta^{18}\text{O}$  值则由降水量和蒸发比(P/E)和入湖水体  $\delta^{18}\text{O}$  值控制(Horton et al., 2016)。在湖水补给恒定的情况下,P/E 值越大,气候越湿润, $\delta^{18}\text{O}$  值越偏负,反之则越偏正。另一方面,湖相碳酸盐岩碳同位素值主要与湖水中溶解无机碳的碳同位素组分变化一致,而湖水溶解无机碳同位素又受到集水盆地注入水的碳同位素、湖水面大气  $\text{CO}_2$  的交换率、生物生命活动、水生和陆源有机质降解和再循环速率、湖水蒸发作用等因素影响(Romanek et al., 1992);例如,当湖水补给量减少时,湖泊面积减小、湖水滞留时间延长,湖水中溶解的  $^{13}\text{C}$  浓度增高;湖泊中藻类植物的光合

作用也会造成湖泊水中的碳同位素正偏(Leng and Marshall, 2004)。此外,湖相碳酸盐岩碳氧同位素的相关性关系在一定程度上能反映当时的沉积环境。Talbot(1990)发现封闭型半咸水—咸水湖原生碳酸盐岩的  $\delta^{13}\text{C}$  值和  $\delta^{18}\text{O}$  值呈正相关关系( $R>0.7$ ),且随着湖水量的减少或增加, $\delta^{13}\text{C}$  值和  $\delta^{18}\text{O}$  值会随之变重或变轻,而在开放型湖泊中, $\delta^{13}\text{C}$  值和  $\delta^{18}\text{O}$  值常呈弱相关或无相关关系(Talbot, 1990)。若以  $\delta^{18}\text{O}$  值为横坐标、 $\delta^{13}\text{C}$  值为纵坐标、0 为原点建立坐标系,开放型淡水湖泊投点一般落在第二、三象限, $\delta^{18}\text{O}$  值以负值为特征,且  $\delta^{18}\text{O}$  值变化范围相对狭窄,碳氧同位素多为不相关,少数呈弱相关;而封闭型咸水湖泊其投点大多数落于第一、二象限, $\delta^{18}\text{O}$  正负值均有,变化范围相对较宽,两者相关性明显,且相关系数大小代表封闭性的强弱;对于半开放—半封闭型湖泊,其投点大多数落于第二象限, $\delta^{18}\text{O}$  与  $\delta^{13}\text{C}$  呈弱相关性或中等相关(杨国臣, 2010)。同时,由碳氧同位素获得的古环境及其变化也可以由碳酸盐岩层中的矿物组成进一步佐证,



注:所有氧同位素值均采用方解石和白云石氧同位素分馏系数校正数据

图5 沱沱河盆地阿布日阿加宰剖面湖相碳酸盐岩碳氧同位素曲线与气候背景分析

Fig. 5 Carbon and oxygen isotope curves and climatic analysis of the APC section, Tuotuohe Basin

通常湖泊碳酸盐岩矿物的种类与水体的盐度密切相关,当蒸发作用较强时白云石才会出现。因此,我们引用白云石比值“白云石/(方解石+白云石)” (图 5)来作为蒸发作用强弱的替代指标(Fang et al., 2022)。

考虑到不同类型碳酸盐矿物的碳氧同位素分馏会造成同位素值存在偏差(Leng and Marshall, 2004),因此在进行碳氧同位素特征分析之前,要对所测算的同位素值进行校正。通常认为,反应过程中,碳元素完全转换为  $\text{CO}_2$ ,不存在碳同位素分馏,只需对氧同位素值进行校正(Swart et al., 1991)。本文样品中碳酸盐矿物为方解石与白云石,使用分馏系数  $\alpha_{\text{方解石}}=1.010250$ (Friedman and O'Neil, 1977; Swart et al., 1991)和  $\alpha_{\text{白云石}}=1.011934$ (Rosenbaum and Sheppard, 1986)对氧同位素值进行校正,方解石-白云石的相对百分比含量由 X 射线衍射物相结论确定,校正后的  $\delta^{18}\text{O}$  值见表 1。根据阿布日阿加宰剖面湖相碳酸盐岩中碳氧同位素组成特征分析,将沱沱河盆地新生代湖泊水文状态和气候背景划分为四个阶段(图 5):

(1)第一阶段为剖面沱沱河组至雅西措组下部冲洪积扇相—河流相沉积时期,时代介于 38.5~

30.5 Ma。该阶段  $\delta^{13}\text{C}$  值为整个剖面最高值,  $\delta^{18}\text{O}$  值为整个剖面最低值,  $\delta^{13}\text{C}$  值变化范围为  $-0.81\text{‰} \sim +5.43\text{‰}$ , 均值为  $+2.42\text{‰}$ ,  $\delta^{18}\text{O}$  值变化范围为  $-10.26\text{‰} \sim -6.65\text{‰}$ , 整体相对稳定,均值为  $-8.29\text{‰}$ 。投点多落入第二象限,少数落入第三象限,碳氧同位素呈不相关(图 6),以发育开放性湖泊为特征,白云石比值整体较低(图 5),显示该时期降水较丰富,蒸发作用相对较弱,气候相对湿润。该认识与 Cyr et al.(2006)和伊海生等(2007)采自二道沟同时期湖相碳酸盐岩碳氧同位素和 Ca/Mg 数据所反映的湿润气候条件一致。但需要指出的是,古纬度及孢粉数据则表明该时期沱沱河盆地处于副热带高压气候带内,气候以暖干气候为主(段志明等, 2007; Miao et al., 2016; 李乐意等, 2022),这似乎与湖相碳酸盐岩碳氧同位素及矿物组合所揭示的古气候背景相矛盾,但是仔细研究不难发现,本次研究的湖相碳酸盐岩样品取自冲积扇—河流相间歇性湖泊相砂质灰岩和含生物碎屑泥晶灰岩,指示干旱气候背景下间歇性湿润气候期的存在。晚始新世时期(约 35 Ma),可可西里地区古纬度约为北纬  $26^\circ$ ,整体处于副热带高压气候带内(李乐意等, 2022),与现代地中海气候情况类似,在冬季和全球

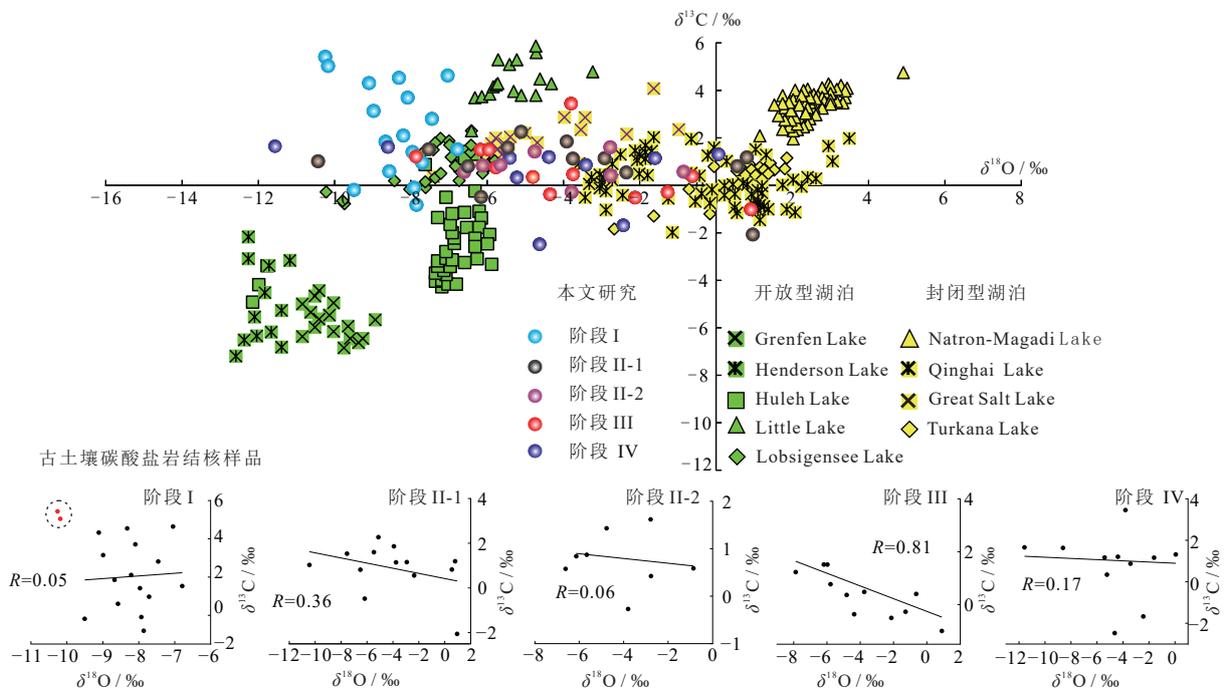


图 6 研究区碳酸盐岩与现代封闭型湖泊和开放性湖泊沉积碳酸盐岩  $\delta^{13}\text{C}$  和  $\delta^{18}\text{O}$  值比较 (数据引用自 Talbot, 1990; Talbot et al., 1990)

Fig. 6 Comparison of  $\delta^{13}\text{C}$  and  $\delta^{18}\text{O}$  of the carbonate rocks in the APC section of the Tuotuohe Basin with those from modern closed lakes and open lakes (data was sourced from Talbot, 1990; Talbot et al., 1990)

降温期间,西风带与副热带高压带中间的过渡带会向南迁移,甚至能够达到高原北部可可西里、囊谦地区(Fang et al., 2022)。现代的青藏高原中部至少存在两个主要水分源,即南亚季风和西风带(图1a; Li and Garziona, 2017),研究表明,晚渐新世时期位于可可西里盆地南侧的冈底斯和羌塘山脉海拔高程均已超过4 000 m(Wang et al., 2008; Xu et al., 2013),特别是晚始新世(44~40 Ma)羌塘中央分水岭山脉的形成几乎完全阻挡了南亚季风向北输送的路径(Ding et al., 2014; Xiong et al., 2020; Zhang et al., 2021);相反,可可西里及其北侧的柴达木盆地、祁连山、天山等山系均处于低海拔(<2 000 m)区域,西风仍控制着整个东亚中纬度地区(Cui et al., 2023),因此,该时期的湿润气候极可能是受到西风间歇性的雨水输入所致。这也得到了氧同位素组成的进一步证明,一方面,现代西风带一般具较轻的雨水氧同位素值,年平均氧同位素值为-11‰~-7‰(Han et al., 2014; Caves et al., 2015),该值与沱沱河组和雅西措组下部氧同位素值(-10.26‰~-6.65‰)基本相当。另一方面,Fang et al. (2022)系统总结了高原北部受西风带控制区域(例如柴达木盆地、贵德盆地、门源盆地等)的新生代湖相碳酸盐岩的碳氧同位素特征(表2),结果发现它们无一例外地表现出与西风带雨水相

似的氧同位素值,由此提出晚始新世青藏高原北部仍接受了来自西风带的雨水输入的观点。因此,晚始新世可可西里地区在干旱气候背景下存在间歇性西风带雨水输入的湿润性气候条件。

(2)第二个阶段对应于雅西措组中上部浅湖相沉积阶段,时代大致介于30.5~23.6 Ma,该阶段26.5 Ma前后碳氧同位素特征存在明显变化,其中30.5~26.5 Ma时期(图5, II-1), $\delta^{13}\text{C}$ 值变化介于-2.06‰~+2.27‰(平均值为+0.88‰), $\delta^{18}\text{O}$ 值变化介于-8.80‰~+1.12‰(平均值为-3.42‰),变化幅度较大,碳同位素显著降低(偏移量1.54‰),氧同位素则明显正偏(+4.87‰)。造成湖泊碳酸盐岩氧同位素正偏、碳同位素负偏的原因有三种(Fontes et al., 1996; 曹高社等, 2019):一是平均温度的升高有利于植被生长及土壤活动的发展,在这种条件下,降水 $\delta^{18}\text{O}$ 值偏正,导致沉淀的碳酸盐矿物 $\delta^{18}\text{O}$ 值偏正, $\delta^{13}\text{C}$ 值则因植被和土壤带来较轻的 $\delta^{13}\text{C}$ 值而整体偏负;二是湖泊内生物活动消减了由湖水溶解无机碳与大气 $\text{CO}_2$ 的交换作用所带来的影响, $\delta^{18}\text{O}$ 值因蒸发作用而升高, $\delta^{13}\text{C}$ 值因生物源 $\text{CO}_2$ 的释放而明显降低;三是湖泊底部环境发生了由还原环境到氧化环境的转变,有机质被氧化后会产生同位素较轻的 $\text{CO}_2$ ,使得沉淀的碳酸盐矿物 $\delta^{13}\text{C}$ 值偏负。由于雅西措组地层中缺乏植物化石且沉积时期呈

表2 剖面古土壤结核与西风带气候区碳酸盐岩样品碳氧同位素值对比

Table 2 Comparison of carbon and oxygen isotope values between paleosol nodules in APC section and carbonate samples in the westerlies-dominated climate

位置	剖面	$\delta^{18}\text{O}_{\text{VPDB}} / \text{‰}$	$\delta^{13}\text{C}_{\text{VPDB}} / \text{‰}$	岩性	样品数量/件	地层	参考文献
沱沱河盆地	阿布日阿加宰	-10.22	+5.24	古土壤结核	2	沱沱河组	本研究
		-9.57	-5.6	古土壤结核	2	路乐河组	Fang et al., 2022
	红柳沟	-10.29	-1.72	碳酸盐胶结物	3	路乐河组	Fang et al., 2022
		-9.93	-3.71	古土壤结核	5	路乐河组	Fang et al., 2022
		-11.79	-2.4	碳酸盐胶结物	1	路乐河组	Fang et al., 2022
柴达木盆地	红沟	-9.7	-7.1	古土壤结核	95	路乐河组	Song et al., 2018
		-11.1		碳酸盐胶结物	4	路乐河组	Graham et al., 2005
		-11.1	-5.7	碳酸盐胶结物	23	路乐河组	Kent-Corson et al., 2009
		-10.3	-5.7	碳酸盐胶结物	11	路乐河组	Kent-Corson et al., 2009
贵德盆地	尕让	-10.95	-5.56	古土壤结核	6	西宁群	Fang et al., 2022
门源盆地	东川	-10.73	-2.2	碳酸盐胶结物	2	西宁群	Fang et al., 2022
塔里木盆地	阿尔塔什	-7.8	-3.3	灰岩	6		Kent-Corson et al., 2009
酒泉盆地	喀什塔什	-14.5		碳酸盐胶结物	9		Graham et al., 2005
	火烧沟	-8.9	-2.6	古土壤结核	5	火烧沟组	Fang et al., 2022

干冷的气候特征(段志明等, 2007), 排除气温增加导致植被和土壤带来较轻的  $\delta^{13}\text{C}$  值的可能性, 而湖泊水体较浅, 因此也不存在湖底由还原环境向氧化环境变化的情况。沱沱河盆地雅西措组发育硫酸盐矿物—石膏(伊海生等, 2009; Li et al., 2012; Staisch et al., 2016), 在湖水硫酸盐含量高的情况下, 硫酸盐还原菌的还原作用能使有机质氧化, 将大量较轻  $\delta^{13}\text{C}$  值的  $\text{CO}_2$  和  $\text{HCO}_3^-$  释放于湖水中, 导致沉淀的碳酸盐矿物  $\delta^{13}\text{C}$  值偏负(杨晓璇等, 2022; Zeng et al., 2023), 因此我们认为, 该时期碳酸盐矿物中  $\delta^{13}\text{C}$  值偏负可能是硫酸盐还原菌还原作用导致的。该时期碳氧同位素投点多落于第二象限, 少数落于第一象限与第四象限(图 6), 显示为半开放—半封闭型湖泊特征, 碳氧同位素呈弱相关(图 6), 同时白云石比值在垂向上明显增加(图 5), 代表大气降水量减少, 蒸发作用增强, 气候由第一阶段干旱背景下相对湿润气候条件向该时期干旱气候的转变。孢粉学和古盐度资料也记录了这次气候转型(段志明等, 2007; 段其发等, 2008; 李建国, 2015; 李乐意, 2019; Li et al., 2023b)。造成这种气候转变的原因可能有二: 第一, 在早始新世—中始新世, 可可西里盆地是统一的大盆地(Dai et al., 2012), 沉积了一套以冲积扇相—河流相的风火山组和沱沱河组地层, 而到了始新世—渐新世, 盆地上地壳缩短及风火山逆冲断层在中—晚始新世的活动(Staisch et al., 2016)将统一的可可西里盆地分割为多个小的次级盆地, 雅西措组沉积在各个次级盆地之中, 这一过程可能导致沱沱河盆地水文状态、沉积环境发生明显改变(刘志飞等, 2005), 研究剖面湖泊相沉积环境由洪泛平原内部的间歇性湖泊转变为永久性湖泊; 第二, 与沱沱河盆地局部隆升有关。前人的研究表明, 晚渐新世, 沱沱河盆地及相邻地区发生了强烈的地壳缩短, 构造活动发生在雅西措组沉积之后(刘志飞等, 2001; Wang et al., 2002), 该地区海拔高程在此时期发生了显著抬升, 由晚始新世的  $<2\ 000\ \text{m}$ (Cyr et al., 2006; Miao et al., 2016)上升到早渐新世(29 Ma)的  $3\ 000\ \text{m}$  左右(Song et al., 2021; Li et al., 2023b)。但需要强调的是, 参照 Fang et al. (2022)对于高原北缘不同高程氧同位素衰减梯度 ( $-1.3\text{‰}/\text{km}$ ) 测算, 可可西里地区  $1\ 000\ \text{m}$  的隆升幅度不足以导致此阶段高达  $4.87\text{‰}$  的正偏移量。因此, 比较好的解释是晚渐新世高原北部地区的区域隆升和随之所带来的可可西里地区湖泊水文状态

的改变, 这两者共同作用致使该阶段氧同位素相对正偏。

其后在  $26.5\sim 23.6\ \text{Ma}$  时期(图 5, II-2),  $\delta^{13}\text{C}$  值变化范围为  $-0.27\text{‰}\sim +1.62\text{‰}$ , 均值为  $+0.76\text{‰}$ ,  $\delta^{18}\text{O}$  值变化范围为  $-6.13\text{‰}\sim +0.73\text{‰}$ , 均值为  $-3.37\text{‰}$ 。相较于 II-1 时期, 碳同位素值变化不大, 均值仅下降  $0.12\text{‰}$ , 氧同位素均值虽然仅微弱增加 ( $0.05\text{‰}$ ), 但在底部氧同位素值显著降低, 由下部的  $+1.12\text{‰}$  降到  $-6.13\text{‰}$ , 随后开始出现正偏移趋势(图 5)。碳氧同位素投点分散, 波动幅度显著, 大部分落于第二象限, 少数落于第三象限, 碳氧同位素相关性差(图 6), 以半封闭半开放型湖泊为特征。虽然氧同位素均值出现微弱降低, 但其仍处于相对高值且整体正偏, 同时白云石比值在该阶段增加(图 5), 整体代表了蒸发作用相对增加, 气候相对干冷。造成这一气候转变的原因可能与该时期青藏高原北缘普遍存在的构造活动有关。前人研究显示, 位于可可西里以西的天山、西昆仑、帕米尔高原等地区在该时期发生普遍隆升。例如, 来自新疆阿尔塔什地区碎屑锆石 U-Pb 地质年代学物源分析研究表明, 在约  $25\ \text{Ma}$  时物源发生了重大变化, 这既可以归因于西昆仑内古排水模式的变化, 也可以归因于由西昆仑和北帕米尔的初始抬升所导致的地形改变(Blayney et al., 2016; Yang et al., 2018); Wang et al. (2020)通过土壤碳酸盐稳定氧同位素值分析, 同样提出自  $25\ \text{Ma}$  以来帕米尔—天山造山带很大一部分充当了西风带的水分屏障, 并在推动亚洲干旱化中发挥了重要作用; 最近 Li et al. (2023)通过研究区北部的东昆仑山脉低温热年代学研究表明, 在  $27\sim 25\ \text{Ma}$ , 山体发生了显著隆升。另一方面, 前人研究显示, 该时期也是可可西里地区地形起伏比较明显的阶段(Li and Garziona, 2023), 古海拔已经进一步上升至  $3\ 400\sim 4\ 200\ \text{m}$ (Polissar et al., 2009), 上地壳缩短变形基本停止(Staisch et al., 2014; 李乐意, 2019), 而位于可可西里地区北部的阿尔金山、祁连山和昆仑山在该时期也发生了快速剥露(Jian et al., 2018; He et al., 2021; Wu et al., 2021a; Wu et al., 2021b), 加之西宁、贵德、兰州和柴达木盆地也开始形成锥形(Dai et al., 2006; Wang et al., 2016; Fang et al., 2019; Xia et al., 2021)。因此, 晚渐新世是青藏高原北部地区地貌格局发生重大转变的时期, 一方面, 研究区西部包括帕米尔—天山、昆仑山等高原西北部地貌格局发生重大改变, 可能阻挡

了西风带水汽向东输入的路径而导致研究区出现更加干旱的气候条件;而另一方面,高原北部包括可可西里、昆仑山、祁连山等重大山系以及西宁、贵德、兰州和柴达木盆地等山间盆地均发生不同程度的隆升,导致区域水文状态发生了重大改变,高原性气候雏形开始出现,气候变得更加干冷,研究剖面的气候系统也在 26.5 Ma 前后由整体湿润向急剧干冷转变。

(3)第三阶段对应于五道梁组下部浅湖相沉积,时代介于 23.6~22.3 Ma。该阶段  $\delta^{13}\text{C}$  值变化范围为  $-0.10\text{‰}\sim+1.51\text{‰}$ , 均值为  $+0.38\text{‰}$ ,  $\delta^{18}\text{O}$  值变化范围为  $-7.88\text{‰}\sim+0.90\text{‰}$ , 均值为  $-3.81\text{‰}$ 。碳氧同位素投点分散,波动幅度显著,多数落于第二象限,少数落于第三、四象限(图 6),氧同位素值处于相对高值,显示为半开放—半封闭型湖泊特征,碳氧同位素相关性较强(图 6)。虽然氧同位素均值相对第二阶段正偏  $+0.85\text{‰}$ ,但对比第二阶段上部样品的氧同位素值来看,该阶段样品中氧同位素值存在一个小规模的负偏,同时白云石比值在该阶段也显著降低(图 5),表明该阶段大气降水量相对增加,存在短暂性湖泊水体的输入,蒸发作用相对降低,气候相对湿润,该时期湿润的气候在临近地区也有体现(吴珍汉等, 2006, 2009)。此外,伊海生等(2009)在距离剖面东南约 20 km 的通天河剖面利用泥质岩硼含量重建的雅西措组和五道梁组沉积时期古盐度变化结果也显示,在五道梁组沉积的早期,沱沱河盆地出现淡水沉积环境,气候相对湿润。因此在五道梁沉积的早期,可可西里地区出现了湿润气候,造成这一湿润气候的原因可能与当时的古地理背景相关,前人的研究表明,在始新世到渐新世,可可西里地区发育有五道梁、北麓河、沱沱河、通天河和东温泉湖盆等多个小的次级湖盆(Staisch et al., 2016),而到了中新世早期,这些湖盆相继接通并形成了一个巨大的可可西里“古大湖”,面积甚至超过了  $100000\text{km}^2$ (吴珍汉等, 2006; Wu et al., 2008),大规模古大湖的突然出现意味着该地区雨水增多,气候湿润。

(4)第四个阶段对应于五道梁组上部干盐湖相沉积时期(22.3~19.7 Ma),  $\delta^{13}\text{C}$  值变化于  $-2.47\text{‰}\sim+3.46\text{‰}$ 之间,平均值为  $+0.79\text{‰}$ ,  $\delta^{18}\text{O}$  值变化范围为  $-11.58\text{‰}\sim+0.06\text{‰}$ , 均值为  $-4.64\text{‰}$ ,碳同位素均值相对第三阶段正偏  $+0.41\text{‰}$ ,整体处于负偏趋势,氧同位素均值相对上阶段偏负  $0.83\text{‰}$ ,碳氧同位素

投点多数落于第二象限,少数落于第三象限(图 6),虽然氧同位素值相比上阶段偏负,但垂向上具有正偏趋势,同时白云石比值逐渐增大(图 5),结合五道梁组地层顶部出现大量石膏沉积的情况,认为该时期湖泊类型已经转变为封闭型湖泊(周昱昱等, 2007)。需要注意的是,阿布日阿加宰剖面五道梁组所测定的碳同位素组成与伊海生等(2007)在五道梁和通天河剖面分析的湖相碳酸盐岩出现的正偏趋势存在明显差异,造成这种差异的主要原因可能有二,其一为伊海生等人在其研究剖面中见大量叠层石,藻类活动能够导致湖泊碳酸盐岩碳同位素出现正偏;其二与本研究层段出现的大量石膏沉积导致有机质降解,使之呈现负偏移现象有关。整体来说,该时期较高的  $\delta^{18}\text{O}$  值及大套干盐湖沉积体系的发育意味着强烈蒸发作用和干旱气候条件的存在,这也得到了前人孢粉学和古气候研究结论的支持。在格拉丹东西美杜塘剖面,段其发等(2008)发现,在雅西措组上部到五道梁组下部地层中喜凉和耐寒的针叶林含量明显增加,同时蔡熊飞等(2008)的研究则表明在可可西里盆地五道梁组底部开始出现代表寒冷和干旱气候的裸子植物植硅体,李乐意(2019)研究显示,该剖面代表寒冷干旱的冷杉、云杉和松属(*Abies+Picea+Pinus*)组分在五道梁组地层中含量突增,研究团队前期在该地区报道的早中新世两次  $\text{C}_4$  植被的扩张和云杉化石的出现,也进一步证实青藏高原北部在该时期发生过降温 and 干旱化过程(Wu et al., 2019)。这一气候转变可能与可可西里地区进入高原系统以及亚洲内陆干旱化有关:一方面,如上所述,前人对古海拔高程的重建结果已经显示了早在雅西措组沉积的晚期至五道梁组沉积早期,可可西里盆地古海拔已经达到甚至超过  $4000\text{m}$ (吴珍汉等, 2007; Polissar et al., 2009; 王成善等, 2009),与现代青藏高原永久性大陆冰川( $>4000\text{m}$ , Hock et al., 2019)和多年冻土( $>3000\text{m}$ , Hock et al., 2019)分布区的海拔高度基本一致,意味着可可西里盆地显然已经进入高原气候系统,区域气候寒冷、干旱;另一方面,前人对亚洲内陆干旱化演化记录做了大量的研究,早期认为,22 Ma 即为亚洲内陆干旱化开始的时间,在青藏高原以北的兰州、西宁、贵德、柴达木等地自此开始大面积出现风尘黄土沉积(Guo et al., 2002; Qiang et al., 2011; Yang et al., 2013; Fang et al., 2015; Liu et al., 2021),其后 Sun et al. (2010)对准噶尔盆地、

Zheng et al. (2015)对塔里木盆地塔克拉沙漠最早的风尘沉积年代学研究,以及最近 Jia et al. (2020)对青藏高原北缘大范围新生代沉积盆地的孢粉学研究均指示了该时期亚洲内陆干旱化的形成和加剧,可可西里地区大面积出现的巨厚五道梁组膏岩沉积及相应的碳氧同位素特征所指示的干旱气候背景,可能就是这种干旱化气候的重要响应。

## 5 结论

(1)沱沱河盆地新生代湖相碳酸盐岩主要分布于始新世至中新世的沱沱河组、雅西措组和五道梁组,野外以灰白色、黄灰色色调为主,多以薄层状产出为特征,与紫红色砂泥岩层对比鲜明。岩石学特征表明,该地区碳酸盐岩岩性主要为泥微晶灰岩,以及少量白云岩和含生物碎屑灰岩。

(2)碳氧同位素构成及特征演化揭示的该地区气候变化历史:38.5~30.5 Ma,气候相对湿润,是干旱气候背景下西风带间歇性降水输入导致;30.5~26.5 Ma 时期气候相对湿润,但区域降水量减少,蒸发作用加强,与高原北部局部隆升及湖盆水文状态发生改变有关,26.5~23.6 Ma 时期,蒸发作用相对增强,气候干冷,是青藏高原北部地区地貌格局发生转变、西风带降水输入减少导致;23.6~22.3 Ma,气候相对湿润,与青藏高原腹地发育古大湖有关;22.3~19.7 Ma,气候更加干冷,湖泊类型转变为封闭型咸水湖,为可可西里地区进入高原系统和亚洲内陆干旱化所致。因此,沱沱河盆地始新世—中新世湖泊水文状态和气候背景的转变与高原北部古地理格局和地貌演化存在极大关联。

**致谢:** 剖面实测和样品采集得到陈云博士、樊秋爽硕士、包万铖硕士的帮助,两名匿名审稿专家对本文提出了宝贵且中肯的意见和建议,在此一并表示感谢。

## References

- An Z S, John E K, Warren L P, et al., 2001. Evolution of Asian monsoons and phased uplift of the Himalaya-Tibetan plateau since Late Miocene times[J]. *Nature*, 411 (6833): 62.
- Bao W C, Xia G Q, Lu C, et al., 2023. Late Eocene to early Oligocene geochemical characteristics and paleoclimatic significance of the second member of Niubao Formation in the Lunpola Basin, Tibet[J]. *Sedimentary Geology and Tethyan Geology*, 43 (3): 580 - 591 (in Chinese with English abstract).
- Blayney T, Najman Y, Dupont - Nivet G, et al., 2016. Indentation of the Pamirs with respect to the northern margin of Tibet: Constraints from the Tarim basin sedimentary record[J]. *Tectonics*, 35 (10): 2345 - 2369.
- Cai X F, Liu D M, Wei Q R, et al., 2008. Characteristics of North of Tibetap Plateau uplift at Paleocene-Miocene—The evidence from Ke Kexili Basin[J]. *Acta Geologica Sinica*, 28 (2): 194 - 203+291 - 292 (in Chinese with English abstract).
- Cao G S, Yu S J, Sun F Y, et al., 2019. Carbon and oxygen isotopic composition and palaeoenvironment analysis of lacustrine carbonate rocks in the upper member of Early Triassic Sunjiagou Formation, Yiyang area, western Henan Province[J]. *Acta Geologica Sinica*, 93 (5): 1137 - 1153 (in Chinese with English abstract).
- Caves J K, Winnick M J, Graham S A, et al., 2015. Role of the westerlies in Central Asia climate over the Cenozoic[J]. *Earth and Planetary Science Letters*, 428: 33 - 43.
- Cui J W, Li Z H, Dong X P, et al., 2023. Paleogene-Neogene environmental evolution and the uplift-sedimentation response of the NE Tibetan Plateau[J]. *Terra Nova*, 36 (2): 112 - 125.
- Cyr A J, Currie B S, Rowley D B, 2006. Geochemical evaluation of Fenghuoshan group lacustrine carbonates, north-central Tibet: Implications for the paleoaltimetry of the Eocene Tibetan Plateau[J]. *Journal of Geology*, 113 (5): 517 - 533.
- Dai J G, Zhao X X, Wang C S, et al., 2012. The vast proto-Tibetan Plateau: New constraints from Paleogene Hoh Xil Basin (Article) [J]. *Gondwana Research*, 22 (2): 434 - 446.
- Dai S, Fang X M, Dupont - Nivet G, et al., 2006. Magnetostratigraphy of Cenozoic sediments from the Xining Basin: Tectonic implications for the northeastern Tibetan Plateau[J]. *Journal of Geophysical Research: Solid Earth*, 111 (B11).
- Deng W F, Wei G J, Li X H, 2005. Online analysis of carbon and oxygen isotopic compositions of impure carbonate[J]. *Geochimica*, 34 (5): 495 - 500 (in Chinese with English abstract).
- Ding L, Xu Q, Yue Y H, et al., 2014. The Andean-type Gangdese Mountains: Paleoelevation record from the Paleocene-Eocene Linzhou Basin[J]. *Earth and Planetary Science Letters*, 392: 250 - 264.
- Duan Q F, Zhang K X, Wang J X, et al., 2008. Oligocene palynoflora, paleovegetation and paleoclimate in the Tanggula mountains, Northern Tibet[J]. *Acta Micropalaeontologica Sinica*, 25 (2): 185 - 195 (in Chinese with English abstract).
- Duan Z M, Li Y, Shen Z W, et al., 2007. Analysis of the evolution of the Cenozoic ecological environment and process of plateau surface uplift in the Wenquan area in the interior of the Qinghai-Tibet Plateau[J]. *Geology In China*, 34 (4): 688 - 696 (in Chinese with English abstract).
- Fang X M, Fang Y H, Zan J B, et al., 2019. Cenozoic magnetostratigraphy of the Xining Basin, NE Tibetan Plateau, and its constraints on paleontological, sedimentological and tectonomorphological evolution[J]. *Earth-Science Reviews*, 190: 460 - 485.
- Fang X M, Guo Z T, Jiang D B, et al., 2022. No monsoon-dominated

- climate in northern subtropical Asia before 35 Ma [J]. *Global and Planetary Change*, 218: 103970.
- Fang X M, Zan J B, Appel E, et al., 2015. An Eocene-Miocene continuous rock magnetic record from the sediments in the Xining Basin, NW China: Indication for Cenozoic persistent drying driven by global cooling and Tibetan Plateau uplift[J]. *Geophysical Journal International*, 201 (1) : 78–89.
- Fontes J C, Gasse F, Gibert E, 1996. Holocene environmental changes in Lake Bangong basin (Western Tibet) . Part 1: Chronology and stable isotopes of carbonates of a Holocene lacustrine core[J]. *Palaeogeography, Palaeoclimatology, Palaeoecology*, 120 (1–2) : 25–47.
- Friedman I, O'neil J R, 1977. Compilation of stable isotope fractionation factors of geochemical interest [R]. U.S. Geological Survey Professional Paper: 1–55.
- Graham S A, Chamberlain C P, Yue Y, et al., 2005. Stable isotope records of Cenozoic climate and topography, Tibetan Plateau and Tarim Basin[J]. *American Journal of Science*, 305 (2) : 101–118.
- Guo Z T, William F R, Hao Q Z, et al., 2002. Onset of Asian desertification by 22 Myr ago inferred from loess deposits in China[J]. *Nature*, 416 (6877) : 159.
- Han W X, Fang X M, Ye C C, et al., 2014. Tibet forcing Quaternary stepwise enhancement of westerly jet and central Asian aridification: Carbonate isotope records from deep drilling in the Qaidam salt playa, NE Tibet[J]. *Global and Planetary Change*, 116: 68–75.
- He P J, Song C H, Wang Y D, et al., 2021. Early Cenozoic activated deformation in the Qilian Shan, northeastern Tibetan Plateau: Insights from detrital apatite fission-track analysis[J]. *Basin Research*, 33 (3) : 1731–1748.
- Hock R, Bliss A, Marzeion B, et al., 2019. GlacierMIP—A model intercomparison of global-scale glacier mass-balance models and projections[J]. *Journal of Glaciology*, 65 (251) : 453–467.
- Hoefs J, 1997. Stable isotope geochemistry [M]. Göttingen: Springer.
- Horton T W, Defliese W F, Tripathi A K, et al., 2016. Evaporation induced <sup>18</sup>O and <sup>13</sup>C enrichment in lake systems: A global perspective on hydrologic balance effects[J]. *Quaternary Science Reviews*, 131: 365–379.
- Hough B G, Garzzone C N, Wang Z, et al., 2010. Stable isotope evidence for topographic growth and basin segmentation: Implications for the evolution of the NE Tibetan Plateau[J]. *Geological Society of America Bulletin*, 123 (1–2) : 168–185.
- Jia Y X, Wu H B, Zhu S Y, et al., 2020. Cenozoic aridification in Northwest China evidenced by paleovegetation evolution[J]. *Palaeogeography, Palaeoclimatology, Palaeoecology*, 557: 109907.
- Jian X, Guan P, Zhang W, et al., 2018. Late Cretaceous to early Eocene deformation in the northern Tibetan Plateau: Detrital apatite fission track evidence from northern Qaidam Basin[J]. *Gondwana Research*, 60: 94–104.
- Kämpf L, Plessen B, Lauterbach S, et al., 2020. Stable oxygen and carbon isotopes of carbonates in lake sediments as a paleoflood proxy[J]. *Geology*, 48 (1) : 3–7.
- Kent-Corson M L, Ritts B D, Zhuang G, et al., 2009. Stable isotopic constraints on the tectonic, topographic, and climatic evolution of the northern margin of the Tibetan Plateau[J]. *Earth and Planetary Science Letters*, 282 (1–4) : 158–166.
- Leng M J, Marshall J D, 2004. Palaeoclimate interpretation of stable isotope data from lake sediment archives[J]. *Quaternary Science Reviews*, 23 (7–8) : 811–831.
- Li C P, Zheng D W, Yu J X, et al., 2023. Late Oligocene mountain building of the East Kunlun Shan in northeastern Tibet: Impact on the Cenozoic climate evolution in East Asia [J]. *Global and Planetary Change*, 224: 104114.
- Li J J, 1999. Studies on the geomorphological evolution of the Qinghai-Xizang (Tibetan) Plateau and Asian monsoon[J]. *Marine geology & Quaternary Geology* (1) : 7–17 (in Chinese with English abstract).
- Li J G, 2015. A Primary Investigation on the Palynassemblages of the Cenozoic Yaxico and Wudaoliang Formations, Hoh Xil[J]. *Quaternary Sciences*, 35 (3) : 787–790 (in Chinese with English abstract).
- Li L Y, 2019. Late Eocene-early Miocene paleoenvironment evolution of the Tuotuohe Basin and its tectonic uplift implications for the central-northern Tibetan Plateau [D]. Beijing: University of Chinese Academy of Sciences (in Chinese with English abstract).
- Li L Y, Chang H, Guan C, 2022. Paleolatitude evolution of the Tuotuohe Basin, central northern Xizang (Tibet) during the Cenozoic and its tectonic, climate implications[J]. *Geological Review*, 68 (5) : 1801–1817 (in Chinese with English abstract).
- Li L Y, Chang H, Farnsworth A, et al., 2023a. Revised chronology of the middle-upper Cenozoic succession in the Tuotuohe Basin, central-northern Tibetan Plateau, and its paleoelevation implications[J]. *Geological Society of America Bulletin*, 136 (5–6) : 2359–2372.
- Li L Y, Chang H, Li X Z, et al., 2023b. Magnetostratigraphy of the Tuotuohe Formation in the Tuotuohe Basin, central-northern Tibetan Plateau: Paleolatitude and paleoenvironmental implications[J]. *Minerals*, 13 (4) : 553.
- Li L, Fan M J, Davila N, et al., 2018. Carbonate stable and clumped isotopic evidence for late Eocene moderate to high elevation of the east-central Tibetan Plateau and its geodynamic implications[J]. *Geological Society of America Bulletin*, 131 (5–6) : 831–844.
- Li L, Garzzone C N, 2017. Spatial distribution and controlling factors of stable isotopes in meteoric waters on the Tibetan Plateau: Implications for paleoelevation reconstruction[J]. *Earth and Planetary Science Letters*, 460: 302–314.
- Li L, Garzzone C N, 2023. Upward and outward growth of north-central Tibet: Mechanisms that build high-elevation, low-relief plateaus [J]. *Science Advances*, 9 (27) : 3058.
- Li Y L, Wang C S, Zhao X X, et al., 2012. Cenozoic thrust system, basin evolution, and uplift of the Tanggula Range in the Tuotuohe region, central Tibet[J]. *Gondwana Research*, 22 (2) : 482–492.
- Li Y L, Wu F R, Liu D J, et al., 2014. Distribution pattern and

- exploration prospect of Longwangmiao Fm reservoirs in the Leshan-Longnüsi Paleouplift, Sichuan Basin[J]. *Natural Gas Industry*, 1 (1) : 72 – 77.
- Liu D S, Zheng M P, Guo Z T, 1998. The origin and development of the Asian monsoon system and its epochal coupling with polar ice sheets and regional tectonic movements[J]. *Quaternary Sciences*, 18 (3) : 194 – 204 (in Chinese with English abstract).
- Liu Y D, Yang Y B, Ye C C, et al., 2021. Global change modulated Asian inland climate since 7.3 Ma: Carbonate manganese records in the western Qaidam Basin [J]. *Frontiers in Earth Science*, 9: 813727.
- Liu Z F, Wang C S, Jin W, et al., 2005. Oligo-Miocene Depositional Environment of the Tuotuohe Basin, Central Tibetan Plateau[J]. *Acta Sedimentologica Sinica*, 23 (2) : 210 – 217 (in Chinese with English abstract).
- Liu Z F, Wang C S, Yi H S, et al., 2001. Reconstruction of Depositional History of the Cenozoic Hoh Xil Basin[J]. *Acta Geologica Sinica*, 75 (2) : 250 – 258 (in Chinese with English abstract).
- Lu C, Xia G Q, Chen Y, et al., 2023. Late Eocene-Early Oligocene clay mineral characteristics and paleoclimate significance in Lunpola Basin, Tibet[J]. *Sedimentary Geology and Tethyan Geology*, 43 (3) : 565 – 579 (in Chinese with English abstract).
- Miao Y F, Wu F L, Chang H, et al., 2016. A Late-Eocene palynological record from the Hoh Xil Basin, northern Tibetan Plateau, and its implications for stratigraphic age, paleoclimate and paleoelevation[J]. *Gondwana Research*, 31: 241 – 252.
- Polissar P J, Freeman K H, Rowley D B, et al., 2009. Paleoaltimetry of the Tibetan Plateau from D/H ratios of lipid biomarkers[J]. *Earth and Planetary Science Letters*, 287 (1 – 2) : 64 – 76.
- Qiang X K, An Z S, Song Y G, et al., 2011. New eolian red clay sequence on the western Chinese Loess Plateau linked to onset of Asian desertification about 25 Ma ago[J]. *Science China (Earth Sciences)*, 54 (1) : 136 – 144.
- Romanek C S, Grossman E L, Morse J W, 1992. Carbon isotopic fractionation in synthetic aragonite and calcite: Effects of temperature and precipitation rate[J]. *Geochimica et Cosmochimica Acta*, 56 (1) : 419 – 430.
- Rosenbaum J, Sheppard S M, 1986. An isotopic study of siderites, dolomites and ankerites at high temperatures[J]. *Geochimica et Cosmochimica Acta*, 50 (6) : 1147 – 1150.
- Shao L Y, Zhang P F, 1991. Stable isotope composition of oxygen and carbon, paleo-salinity and paleo-temperature of carbonate rocks in Heshan Formation, Central Guangxi Province[J]. *Coal Geology of China*, (01) : 25 – 30 (in Chinese with English abstract).
- Shi Y F, Tang M C, Ma Y Z., 1998. Study on the relationship between the second-stage uplift of Qinghai-Tibet Plateau and the breeding of Asian monsoon[J]. *Science In China(Series D)*, (03) : 263 – 271 (in Chinese with English abstract).
- Song B W, Zhang K X, Han F, et al., 2021. Reconstruction of the latest Eocene-early Oligocene paleoenvironment in the Hoh Xil Basin (Central Tibet) based on palynological and ostracod records [J]. *Journal of Asian Earth Sciences*, 217: 104860.
- Song B W, Zhang K X, Zhang L, et al., 2018. Qaidam Basin paleosols reflect climate and weathering intensity on the northeastern Tibetan Plateau during the Early Eocene Climatic Optimum[J]. *Palaeogeography, Palaeoclimatology, Palaeoecology*, 512: 6 – 22.
- Staisch L M, Niemi N A, Clark M K, et al., 2016. Eocene to late Oligocene history of crustal shortening within the Hoh Xil Basin and implications for the uplift history of the northern Tibetan Plateau[J]. *Tectonics*, 35 (4) : 862 – 895.
- Staisch L M, Niemi N A, Hong C, et al., 2014. A Cretaceous - Eocene depositional age for the Fenghuoshan Group, Hoh Xil Basin: Implications for the tectonic evolution of the northern Tibet Plateau[J]. *Tectonics*, 33 (3) : 281 – 301.
- Sun J M, Liu W G, Liu Z H, et al., 2017. Effects of the uplift of the Tibetan Plateau and retreat of Neotethys Ocean on the stepwise aridification of mid-latitude Asian interior[J]. *Bulletin of Chinese Academy of Sciences*, 32 (9) : 951 – 958 (in Chinese with English abstract).
- Sun J M, Ye J, Wu W Y, et al., 2010. Late Oligocene-Miocene mid-latitude aridification and wind patterns in the Asian interior[J]. *Geology*, 38 (6) : 515 – 518.
- Swart P K, Burns S J, Leder J J, 1991. Fractionation of the stable isotopes of oxygen and carbon in carbon dioxide during the reaction of calcite with phosphoric acid as a function of temperature and technique[J]. *Chemical Geology*, 86 (2) : 89 – 96.
- Talbot M R, 1990. A review of the paleohydrological interpretation of carbon and oxygen isotopic-ratios in primary lacustrine carbonates[J]. *Chemical Geology*, 80 (4) : 261 – 279.
- Talbot M R, Kelts K, 1990. Paleolimnological signatures from carbon and oxygen isotopic ratios in carbonates, from organic carbon-rich lacustrine sediments: Chapter 6.
- Wang C S, Liu Z F, Yi H S, et al., 2002. Tertiary crustal shortenings and peneplanation in the Hoh Xil region: implications for the tectonic history of the northern Tibetan Plateau[J]. *Journal of Asian Earth Sciences*, 20 (3) : 211 – 223.
- Wang C S, Zhao X X, Liu Z F, et al., 2008. Constraints on the early uplift history of the Tibetan Plateau[J]. *Proceedings of the National Academy of Sciences of the United States of America*, 105 (13) : 4987 – 4992.
- Wang C S, Dai J G, Liu Z F, et al., 2009. The uplift history of the Tibetan Plateau and Himalaya and its study approaches and techniques: A review[J]. *Earth Science Frontiers*, 16 (3) : 1 – 30 (in Chinese with English abstract).
- Wang S F, Chen Y, Yi H S, et al., 2023. The characteristics of *n*-alkanes from the Palaeogene lacustrine oil shale in the Kanggale area, Nyima Basin, and their paleoenvironment and Paleoclimate significance[J]. *Sedimentary Geology and Tethyan Geology*, 43 (3) : 542 – 554 (in Chinese with English abstract).
- Wang T, Wang Z Q, Yan Z, et al., 2016. Geochronological and geochemical evidence of amphibolite from the Hualong Group, northwest China: Implication for the early Paleozoic accretionary tectonics of the Central Qilian belt[J]. *Lithos*, 248: 12 – 21.

- Wang X, Carrapa B, Sun Y C, et al., 2020. The role of the westerlies and orography in Asian hydroclimate since the late Oligocene[J]. *Geology*, 48 (7) : 728 – 732.
- Wu C, Li J, Ding L, 2021a. Low-temperature thermochronology constraints on the evolution of the Eastern Kunlun Range, northern Tibetan Plateau[J]. *Geosphere*, 17 (4) : 1193 – 1213.
- Wu C, Zuza A V, Li J, et al., 2021b. Late Mesozoic–Cenozoic cooling history of the northeastern Tibetan Plateau and its foreland derived from low-temperature thermochronology[J]. *Geological Society of America Bulletin*, 133 (11–12) : 2393 – 2417.
- Wu C H, Xia G Q, Wagreich M, et al., 2019. Early Miocene expansion of C4 vegetation on the northern Tibetan Plateau[J]. *Global and Planetary Change*, 177: 173 – 185.
- Wu J X, Xia G Q, Chen Y, et al., 2022. Characteristics of clay mineralogy and its paleoclimatic significance across the Oligocene–Miocene transition in the Lunpola Basin, central Tibet[J]. *Acta Sedimentologica Sinica*, 40 (5) : 1265 – 1279 (in Chinese with English abstract).
- Wu Z H, Wu Z H, Ye P S, et al., 2006. Late Cenozoic environmental evolution of the Qinghai-Tibet Plateau as indicated by the evolution of sporopollen assemblages[J]. *Geology In China*, 33 (5) : 966 – 979 (in Chinese with English abstract).
- Wu Z H, Ye P S, Hu D G, et al., 2007. U-Pb isotopic dating of zircons from porphyry granite of the Fenghuoshan Mts, northern Tibetan Plateau and its geological significance[J]. *Geoscience* (3) : 435 – 422 (in Chinese with English abstract).
- Wu Z H, Wu Z H, Hu D G, et al., 2009. Carbon and oxygen isotope changes and palaeoclimate cycles recorded by lacustrine deposits of Miocene Wudaoliang Group in northern Tibetan Plateau[J]. *Geology In China*, 36 (5) : 966 – 975 (in Chinese with English abstract).
- Wu Z H, Barosh P J, Wu Z H, et al., 2008. Vast early Miocene lakes of the central Tibetan Plateau[J]. *Geological Society of America Bulletin*, 120 (9–10) : 1326 – 1337.
- Xiao G Q, Zhang C X, Guo Z T, 2014. Initiation of East Asian monsoon system related to Tibetan Plateau uplift from the latest Oligocene to the earliest Miocene[J]. *Chinese Journal of Nature* (3) : 165 – 169 (in Chinese with English abstract).
- Xia G Q, Wu C H, Li G J, et al., 2021. Cenozoic growth of the Eastern Kunlun Range (northern Tibetan Plateau) : evidence from sedimentary records in the southwest Qaidam Basin[J]. *International Geology Review*, 63 (6) : 769 – 786.
- Xiong Z Y, Ding L, Spicer R A, et al., 2020. The early Eocene rise of the Gonjo Basin, SE Tibet: From low desert to high forest [J]. *Earth and Planetary Science Letters*, 543: 116312.
- Xu Q, Ding L, Zhang L Y, et al., 2013. Paleogene high elevations in the Qiangtang Terrane, central Tibetan Plateau[J]. *Earth and Planetary Science Letters*, 362: 31 – 42.
- Yang G C, 2010. Methods of using carbon-oxygen isotopic characteristics of lacustrine and authigenic carbonates to analyze types of paleolakes: Problems needing attention, the essential points, analytical programs in practical application[J]. *Xinjiang Geology*, 28 (2) : 222 – 227 (in Chinese with English abstract).
- Yang W, Fu L, Wu C D, et al., 2018. U-Pb ages of detrital zircon from Cenozoic sediments in the southwestern Tarim Basin, NW China: Implications for Eocene–Pliocene source-to-sink relations and new insights into Cretaceous–Paleogene magmatic sources[J]. *Journal of Asian Earth Sciences*, 156: 26 – 40.
- Yang X X, Li X F, Guo J J, et al., 2022. Characteristics and significance of C-O isotopes of Oligocene Miocene lacustrine carbonate rocks in Zhangxian, northern margin of west Qinling Mountains[J]. *Northwestern Geology*, 55 (2) : 106 – 115 (in Chinese with English abstract).
- Yang Y B, Fang X M, Appel E, et al., 2013. Late Pliocene–Quaternary evolution of redox conditions in the western Qaidam paleolake (NE Tibetan Plateau) deduced from Mn geochemistry in the drilling core SG-1[J]. *Quaternary Research*, 80 (3) : 586 – 595.
- Yi H S, Lin J H, Zhou K K, et al., 2007. Carbon and oxygen isotope characteristics and palaeoenvironmental implication of the Cenozoic lacustrine carbonate rocks in northern Qinghai-Tibetan Plateau[J]. *Journal of Palaeogeography*, 9 (3) : 303 – 312 (in Chinese with English abstract).
- Yi H S, Shi Z Q, Zhu Y T, et al., 2009. Reconstruction of paleosalinity and lake-level fluctuation history by using boron concentration in lacustrine mudstones[J]. *Journal of Lake Sciences* 21 (1) : 77 (in Chinese with English abstract).
- Zeng L Q, Gatjen J, Reinhardt M, et al., 2023. Extremely <sup>13</sup>C-enriched dolomite records interval of strong methanogenesis following a sulfate decline in the Miocene Ries impact crater lake[J]. *Geochimica Et Cosmochimica Acta*, 362: 22 – 40.
- Zhang J, Liu Y G, Fang X M, et al., 2021. Elevation of the Gangdese mountains and their impacts on Asian climate during the late Cretaceous—A modeling study[J]. *Frontiers in Earth Science*, 9: 810931.
- Zheng H B, Wei X C, Tada R J, et al., 2015. Late Oligocene-early Miocene birth of the Taklimakan Desert[J]. *Proceedings of the National Academy of Sciences of the United States of America*, 112 (25) : 7662 – 7667.
- Zhong D L, Ding L, 1996. Study on uplift process and mechanism of Qinghai-Tibet Plateau[J]. *Science in China (Series D)*, 26 (4) : 289 – 295 (in Chinese with English abstract).
- Shen J, Xue B, Wu J L, et al., 2010. Lake sedimentation and environmental evolution [M]. Beijing: Science Press.
- Zhou K K, Yi H S, Lin J H, 2007. Petrology and sedimentary environments of the lacustrine carbonate rocks from the Miocene Wudaoliang Group in the Hoh Xil Basin, Qinghai[J]. *Sedimentary Geology and Tethyan Geology*, 27 (1) : 25 – 31 (in Chinese with English abstract).

## 附中文参考文献

- 包万铨, 夏国清, 路畅, 等, 2023. 西藏伦坡拉盆地牛堡组二段晚始新世—早渐新世地球化学特征与古气候意义[J]. *沉积与特提斯地质*, 43 (3) : 580 – 591.

- 蔡雄飞, 刘德民, 魏启荣, 等, 2008. 古新世—中新世以来青藏高原北缘隆升的特征——来自可可西里盆地的报告[J]. *地质学报*, 28(2): 194-203+291-292.
- 曹高社, 余爽杰, 孙凤余, 等, 2019. 豫西宜阳地区三叠纪早期孙家沟组上段湖相碳酸盐岩碳氧同位素和古环境分析[J]. *地质学报*, 93(5): 1137-1153.
- 邓文峰, 韦刚健, 李献华, 2005. 不纯碳酸盐碳氧同位素组成的在线分析[J]. *地球化学*, 34(5): 495-500.
- 段其发, 张克信, 王建雄, 等, 2008. 唐古拉山地区渐新世孢粉植物群及其古植被、古气候[J]. *微体古生物学报*, 25(2): 185-195.
- 段志明, 李勇, 沈战武, 等, 2007. 青藏高原腹地温泉地区新生代生态环境演化与高原表面隆升过程分析[J]. *中国地质*, 34(4): 688-696.
- 李吉均, 1999. 青藏高原的地貌演化与亚洲季风[J]. *海洋地质与第四纪地质*(1): 7-17.
- 李建国, 2015. 可可西里新生代雅西措组和五道梁组孢粉组合浅探[J]. *第四纪研究*, 35(3): 787-790.
- 李乐意, 2019. 青藏高原沱沱河盆地晚始新世——早中新世古环境记录及对高原中北部隆升历史的指示意义[D]. 北京: 中国科学院大学.
- 李乐意, 常宏, 关冲, 2022. 青藏高原中北部沱沱河盆地新生代古纬度演化及其对构造和气候的指示意义[J]. *地质论评*, 68(5): 1801-1817.
- 刘东生, 郑绵平, 郭正堂, 1998. 亚洲季风系统的起源和发展及其与两极冰盖和区域构造运动的时代耦合性[J]. *第四纪研究*, 18(3): 194-204.
- 刘志飞, 王成善, 金玮, 等, 2005. 青藏高原沱沱河盆地渐新—中新世沉积环境分析[J]. *沉积学报*, 23(2): 210-217.
- 刘志飞, 王成善, 伊海生, 等, 2001. 可可西里盆地新生代沉积演化历史重建[J]. *地质学报*, 75(2): 250-258.
- 路畅, 夏国清, 陈云, 等, 2023. 西藏伦坡拉盆地晚始新世—早渐新世黏土矿物特征及其古气候意义[J]. *沉积与特提斯地质*, 43(3): 565-579.
- 邵龙义, 张鹏飞, 1991. 桂中合山组碳酸盐岩的氧、碳稳定同位素组成及古盐度和古温度[J]. *中国煤田地质*, (01): 25-30.
- 沈吉, 薛滨, 吴敬禄, 等, 2010. 湖泊沉积与环境演化[M]. 北京: 科学出版社.
- 施雅风, 汤懋苍, 马玉贞, 1998. 青藏高原二期隆升与亚洲季风孕育关系探讨[J]. *中国科学(D辑: 地球科学)*, (03): 263-271.
- 孙继敏, 刘卫国, 柳中晖, 等, 2017. 青藏高原隆升与新特提斯海退却对亚洲中纬度阶段性气候干旱的影响[J]. *中国科学院院刊*, 32(9): 951-958.
- 王成善, 戴紧根, 刘志飞, 等, 2009. 青藏高原与喜马拉雅的隆升历史和研究方法: 回顾与进展[J]. *地学前缘*, 16(3): 1-30.
- 汪素风, 陈云, 伊海生, 等, 2023. 西藏尼玛盆地古近纪湖相油页岩正构烷烃特征及其古环境与古气候意义[J]. *沉积与特提斯地质*, 43(3): 542-554.
- 吴劲宜, 夏国清, 陈云, 等, 2022. 西藏伦坡拉盆地渐新世—中新世之交黏土矿物特征及其古气候意义[J]. *沉积学报*, 40(5): 1265-1279.
- 吴珍汉, 吴中海, 叶培盛, 等, 2006. 青藏高原晚新生代孢粉组合与古环境演化[J]. *中国地质*, 33(5): 966-979.
- 吴珍汉, 叶培盛, 胡道功, 等, 2007. 青藏高原北部风火山花岗斑岩锆石 U-Pb 同位素测年及其地质意义[J]. *现代地质*(3): 435-422.
- 吴珍汉, 吴中海, 胡道功, 等, 2009. 青藏高原北部中新统五道梁群湖相沉积碳氧同位素变化及古气候旋回[J]. *中国地质*, 36(5): 966-975.
- 肖国桥, 张春霞, 郭正堂, 2014. 晚渐新世—早中新世青藏高原隆升与东亚季风演化[J]. *自然杂志*(3): 165-169.
- 杨国臣, 2010. 利用湖泊自生碳酸盐岩氧碳同位素特征分析古湖泊类型的方法——实际应用中的要点及分析程式[J]. *新疆地质*, 28(2): 222-227.
- 杨晓璇, 李雪峰, 郭进京, 等, 2022. 西秦岭北缘漳县中新统一中新统湖相碳酸盐岩碳、氧同位素特征及意义[J]. *西北地质*, 55(2): 106-115.
- 伊海生, 林金辉, 周恩恩, 等, 2007. 青藏高原北部新生代湖相碳酸盐岩碳氧同位素特征及其古环境意义[J]. *古地理学报*, 9(3): 303-312.
- 伊海生, 时志强, 朱迎堂, 等, 2009. 利用泥质岩硼含量重建过去湖泊古盐度和湖面变化历史[J]. *湖泊科学*, 21(1): 77.
- 钟大赉, 丁林, 1996. 青藏高原的隆起过程及其机制探讨[J]. *中国科学: D辑*, 26(4): 289-295.
- 周恩恩, 伊海生, 林金辉, 2007. 可可西里盆地中新统五道梁群湖相碳酸盐岩岩石学特征与沉积环境分析[J]. *沉积与特提斯地质*, 27(1): 25-31.